



UNIVERSITY  
OF WOLLONGONG  
AUSTRALIA

University of Wollongong  
Research Online

---

Faculty of Engineering - Papers (Archive)

Faculty of Engineering and Information Sciences

---

2006

# Second order nonlinear inelastic analysis of composite steel–concrete members. I: theory

Y. L. Pi

*University of New South Wales*

M. A. Bradford

*University of New South Wales*

B. Uy

*University of Wollongong, [brianuy@uow.edu.au](mailto:brianuy@uow.edu.au)*

<http://ro.uow.edu.au/engpapers/183>

---

## Publication Details

This article was originally published as Pi, YL, Bradford, MA and Uy, B, Second Order Nonlinear Inelastic Analysis of Composite Steel–Concrete Members. I: Theory, *Journal of Structural Engineering*, 132(5), May 2006, 751-761. Copyright American Society of Civil Engineers. Original journal available [here](#).

Research Online is the open access institutional repository for the University of Wollongong. For further information contact the UOW Library: [research-pubs@uow.edu.au](mailto:research-pubs@uow.edu.au)

# Second Order Nonlinear Inelastic Analysis of Composite Steel–Concrete Members. I: Theory

Yong-Lin Pi<sup>1</sup>; Mark Andrew Bradford, M.ASCE<sup>2</sup>; and Brian Uy, M.ASCE<sup>3</sup>

**Abstract:** A total Lagrangian finite element (FE) model has been formulated for the nonlinear inelastic analysis of both composite beams and columns. An accurate rotation matrix is used in the position vector analysis and nonlinear strain derivations. The slip between the steel and concrete components due to the flexible shear connection at their interface is considered as an independent displacement in the formulation which makes it easier to assign the corresponding proper slip conditions at the connections between composite beams and columns. The effects of nonlinearities and slip on the deformations and strains in the steel and concrete components, and so on the stress resultants (i.e., internal forces), stiffness, and strength of the composite member are thus combined together in the formulation. The constitutive models for steel and concrete in this investigation are based on the longitudinal normal stress and the shear stress induced by the slip between the steel and concrete components. Hence, these models include the effects of the slip at the interface on the von Mises yield surface, associated flow rule and isotropic hardening rule. These constitutive models can be used in association with any type of uniaxial stress–strain curves for steel and concrete, including hot-rolled or cold-formed steel, and confined or unconfined concrete. The constitutive models are expressed in terms of engineering stresses and strains. The total Lagrangian formulation is applicable for these constitutive models directly, and most convenient for the slips at the interface between the steel and concrete components.

**DOI:** 10.1061/(ASCE)0733-9445(2006)132:5(751)

**CE Database subject headings:** Beams; Columns; Composite materials; Inelastic action; Concrete; Steel; Finite element method.

## Introduction

Structural members with composite steel–concrete sections (Fig. 1), such as composite beams, concrete-filled steel columns, concrete-filled steel arches, composite beams curved in plan, or in space are often used in buildings and bridges. Research on numerical techniques such as finite element (FE) methods for the nonlinear analysis of composite steel–concrete members may have been extensive (Hajjar 1998a, b; Ranzi 2003). FE methods for the nonlinear analysis of composite members may be categorized into two groups: the use of available commercial FE packages; and the development of suitable FE models. When an FE package is used, the steel and concrete components are usually modeled separately using plate, shell, or solid elements and are then assembled together by some connection or interface elements to simulate the shear connectors between the steel and concrete components. Studies by Hirst and Yeo (1980); Thevendran et al. (1999), and

Baskar et al. (2002) belong to this group. Their studies demonstrate that such models are usually quite complicated. For example, several hundred elements are often needed to model a simply supported composite beam (Thevendran et al. 1999; Baskar et al. 2002), and so these models are also computationally intensive. Choosing the right elements for modeling a composite member sometimes is also not easy. For example, Baskar et al. (2002) have shown that the three-dimensional (3D) solid elements in ABAQUS (2003) are not suitable for modeling the concrete components and that, instead, the thick shell elements in ABAQUS should be employed. In addition, it is difficult to properly model the interaction between the steel and concrete components using connector or interface elements available in commercial FE packages such as ABAQUS (2003) and ANSYS (2003). Hence, the slip between the steel and concrete components predicted by these models does not correlate well with experimental results.

In most cases, FE methods for composite members developed by researchers are for composite beams or for concrete-filled tubes (CFT) columns only. FE models that can deal with both composite beams and CFT columns are rarely reported. In terms of methods, FE models can be further classified into force-based (flexibility) formulations and displacement-based (stiffness) formulations. The advantage of force-based formulations is the ease of selecting force interpolation functions that are related to the exact solutions of the governing equations of equilibrium of an element. However, most force-based formulations use force interpolation functions based on the solutions from the governing linear differential equilibrium equations (Spacone 1996); (Salari et al. 1998). Because of this, it is difficult to find force interpolation functions for the interaction between the nonlinear displacements and the internal forces. In order to overcome the difficulty in selecting force interpolation functions that satisfy equilibrium for

<sup>1</sup>Senior Research Fellow, School of Civil & Environmental Engineering, Univ. of New South Wales, Sydney, NSW 2052, Australia. E-mail: y.pi@unsw.edu.au

<sup>2</sup>Professor, School of Civil & Environmental Engineering, Univ. of New South Wales, Sydney, NSW 2052, Australia (corresponding author). E-mail: m.bradford@unsw.edu.au

<sup>3</sup>Professor, School of Civil & Mining Engineering, The Univ. of Wollongong, Wollongong, NSW 2500, Australia. E-mail: brianuy@uow.edu.au

Note. Associate Editor: Sherif El-Tawil. Discussion open until October 1, 2006. Separate discussions must be submitted for individual papers. To extend the closing date by one month, a written request must be filed with the ASCE Managing Editor. The manuscript for this paper was submitted for review and possible publication on April 20, 2004; approved on June 27, 2005. This paper is part of the *Journal of Structural Engineering*, Vol. 132, No. 5, May 1, 2006. ©ASCE, ISSN 0733-9445/2006/5-751–761/\$25.00.

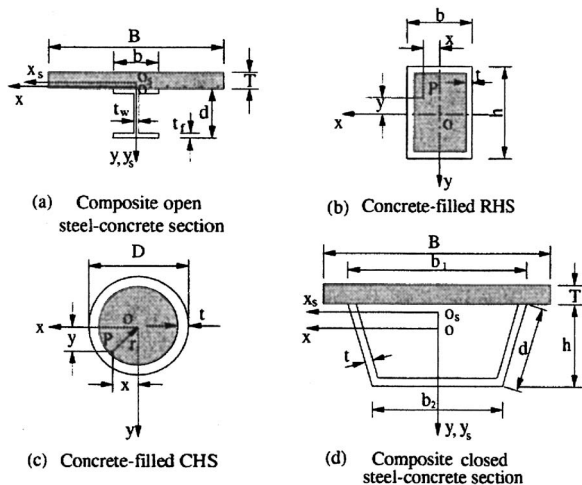


Fig. 1. Composite cross sections

problems with strong interaction between the displacements and the internal forces, a mixed formulation for a nonlinear steel-concrete composite beam element was proposed. Because it is difficult to obtain the exact solutions of the governing equations for the nonlinear equilibrium of an element, force-based formulations do not commonly consider the effects of geometric nonlinearity. Even in the mixed formulations, it appears that the nonlinear axial strain and internal force produced by the second order transverse displacements were not considered.

In a number displacement-based finite element formulations for composite beams, the axial displacements of the steel and concrete components are formulated separately so as to facilitate the slip between the steel and concrete components. The formulations used by Arizumi and Hamada (1981), Daniels and Crisinel (1993), Salari et al. (1998), and Ranzi et al. (2004) belong to this group. Although these models are able to analyze the slip due to the partial interaction between the steel and concrete components, the effects of the slip on strains, stresses, deformations, stiffness, and strength of composite members have often not clearly been demonstrated by these types of models. In addition, most of these models for composite beams assume that the internal axial forces form a force couple that is equal to the bending moment produced by the external transverse loads. The resultant of axial forces in the composite beam is then assumed to be equal to zero. This is correct when the axial internal forces produced by the nonlinear effects of the transverse deformation are not considered. However, the axial internal forces can become significant as the transverse displacements increase. Therefore, these displacement-based formulations often deal with small displacement problems only. They are also prone to the problem of curvature locking (Ranzi et al. 2004), that can occur, with a large stiffness of the shear connection.

FE models for CFT columns have been reported by several researchers. Hajjar et al. (1998a, b) developed a distributed plasticity FE model for concrete-filled steel tube beam-columns. The model considered the interlayer slip and the effect of the slip on CFT beam-column behavior. The model is also suitable for cyclic loading. Lakshmi and Shanmugam (2002) formulated a FE model for nonlinear analysis of CFT columns using yield criteria based on the stress resultants. Other FE models are also reported (Schneider 1988; Shakir-Khalil and Al-Rawdan 1996; Huang et al. 2002; Hu et al. 2003). However, these FE models are

actually models on how to use commercial FE softwares such as ABAQUS.

In addition, in the nonlinear range, the interaction between the slip and in-plane bending will produce additional shear strains and stresses at both the interface and the cross section. These shear strains and stresses have not been addressed in the open literature. The shear stress resultant produced by the shear stresses may be small. However, the shear stresses play a role in the local yield of the steel and concrete and so they should be considered in the FE model. Therefore, the constitutive model for the steel and concrete needs to be based on both the longitudinal normal stresses and the shear stresses induced by the interface slip. Furthermore, as pointed out above, most of the FE models reported in the open literature are specific for composite beams or for the composite columns. Generic FE models that can deal with both composite beams and CFT columns are needed.

The objective of this paper is to present a treatment of a total Lagrangian formulation of a unified FE model for the second order nonlinear inelastic analysis of composite steel-concrete members: both beams and columns, while the companion paper will demonstrate the implementation and application of the FE model.

It is known that updated Lagrangian, total Lagrangian, and corotational formulations are often used for the nonlinear FE model. The stress and strain measures used in these formulations are the second Piola-Kirchhoff stress tensor and the Green-Lagrange strain tensor. Under the small strain assumption, the components of the second Piola-Kirchhoff stress tensor and the Green-Lagrange strain tensor have a physical significance close to that of the conventional engineering stress and strain measures. Because elasto-plastic constitutive models for steel and concrete are usually developed using engineering stress and strain measures, they are directly applicable to the total Lagrangian formulation. The total Lagrangian formulation is conveniently applicable for the constitutive models for the slips at the interface between the steel and concrete components because these models are usually referred to as the undeformed configuration and expressed in a way that is equivalent to engineering stress and strain measures.

In order to present the new FE model in the limited length of this paper, the presentation is concentrated on the theoretical development and some of its applications associated with monotonic loadings. The cyclic behavior and the corresponding topics are not considered in the present study.

## Axis Systems, Rotation, and Curvatures

The basic assumptions for this study are: (1) the Euler-Bernoulli bending theory is used, so that the cross section is assumed to be rigid and local buckling and/or effects of distortion of the cross section are not considered; and (2) the strains are small. Two axis systems are used to describe the geometry of a composite steel-concrete member as shown in Fig. 2. The first set is a body attached (material) right-handed curvilinear orthogonal axis system. In the undeformed configuration, the curvilinear axis system reduces to a rectangular orthogonal axis system in the position  $oyz$ . The axis  $oz$  passes through the centroids of the cross section of the undeformed member and the axis  $oy$  is the minor principal axis of the cross section, as shown in Fig. 2. A unit vector  $\mathbf{p}_z$  in the direction of the centroidal axis  $oz$ , and a unit vector  $\mathbf{p}_y$  in the direction of the axis  $oy$ , form a right-handed orthonormal basis shown in Fig. 2. The unit vectors  $\mathbf{p}_y, \mathbf{p}_z$  are used as the fixed

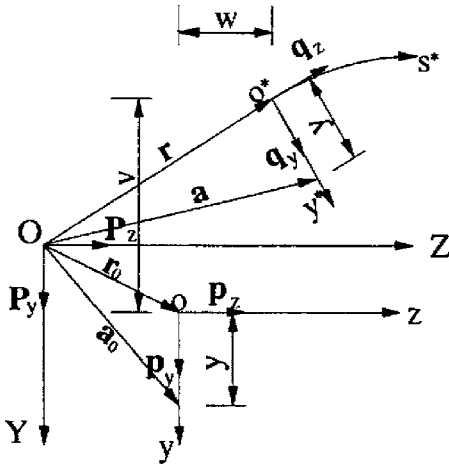


Fig. 2. Axes system, basis, and position vectors

reference basis. They do not change with the deformation.

In the deformed configuration, the centroid  $o$  displaces  $v$ ,  $w$  to the position  $o^*$ , the axis  $oz$  deforms into a curve, and so the body attached curvilinear orthogonal axis system moves and rotates to a new position  $o^*y^*s^*$  as shown in Fig. 2. In the deformed configuration, a unit vector  $\mathbf{q}_z$  is defined along the tangent direction of the deformed centroidal axis  $o^*s^*$ , and the unit vector  $\mathbf{q}_y$  is in the direction of the minor principal axis  $o^*y^*$  of the rotated cross section at  $o^*$ . The unit vectors  $\mathbf{q}_y, \mathbf{q}_z$  also form an orthonormal basis. They attach to the member and move with the member during the deformation with the vector  $\mathbf{q}_z$  remaining normal to the cross section at all times.

A fixed (space) right-handed rectangular coordinate system  $OYZ$  is defined in space as also shown in Fig. 2. The position of the undeformed and deformed member can be defined in the axis system  $OYZ$ . The axes  $OY$  and  $OZ$  are parallel to the axes  $oy$  and  $oz$  of the axes  $oys$  in the undeformed configuration. Unit vectors  $\mathbf{P}_y, \mathbf{P}_z$  in directions  $OY$  and  $OZ$  form a right-handed orthogonal basis.

In the undeformed configuration, the position vector of the centroid  $o$  in the fixed axes  $OYZ$  is  $\mathbf{r}_0$  (Fig. 2), and so the unit vector  $\mathbf{p}_z$  at the centroid  $o$  can be expressed in terms of the position vector  $\mathbf{r}_0$  as (Pi et al. 2003)

$$\mathbf{p}_z = \frac{d\mathbf{r}_0}{dz} \quad (1)$$

In the deformed configuration, the position vector of the centroid  $o^*$  in the fixed axis system  $OYZ$  is  $\mathbf{r}$  as shown in Fig. 2, and so the vector  $\mathbf{q}_z$  tangential to the deformed centroidal axis  $o^*s^*$  can be obtained by differentiating the position vector  $\mathbf{r}$  with respect to the member length  $s^*$  as

$$\mathbf{q}_z = \frac{d\mathbf{r}}{ds^*} = \frac{1}{1+\epsilon} \frac{d\mathbf{r}}{dz} \quad (2)$$

where  $ds^* = (1+\epsilon)dz$  is used, with  $\epsilon$  being the longitudinal normal strain at the centroid.

In the deformed configuration, the position vector  $\mathbf{r}$  of the centroid  $o^*$  can be expressed as (Fig. 2)

$$\mathbf{r} = \mathbf{r}_0 + v\mathbf{p}_y + w\mathbf{p}_z \quad (3)$$

Substituting Eqs. (1) and (3) into Eq. (2) leads to

$$\mathbf{q}_z = \frac{1}{1+\epsilon} \frac{d\mathbf{r}}{dz} = \frac{1}{1+\epsilon} [v'\mathbf{p}_y + (1+w')\mathbf{p}_z] = \hat{v}'\mathbf{p}_y + \hat{w}'\mathbf{p}_z \quad (4)$$

where  $(\ )' \equiv d(\ )/dz$ ,  $\hat{v}' = v'/(1+\epsilon)$ , and  $\hat{w}' = (1+w')/(1+\epsilon)$ .

Because  $\mathbf{q}_z$  is a unit vector, it follows from Eq. (4) that

$$(\hat{v}')^2 + (\hat{w}')^2 = 1 \quad (5)$$

The vector  $\mathbf{q}_z$  can also be expressed as

$$\mathbf{q}_z = \sin \theta \mathbf{p}_y + \cos \theta \mathbf{p}_z \quad (6)$$

where  $\theta$  = angle between the axes  $oz$  and the tangent to the axis  $o^*s^*$ .

In the deformed configuration, according to the Frenet–Serret formulae, the relationship between the derivatives of the basis vectors and the curvatures and twist can be written as (Pi et al. 2003)

$$\frac{d\mathbf{q}_y}{ds^*} = \kappa \mathbf{q}_z = \mathbf{K} \mathbf{q}_y \quad (7)$$

$$\frac{d\mathbf{q}_z}{ds^*} = -\kappa \mathbf{q}_y = \mathbf{K} \mathbf{q}_z$$

where  $\kappa$  = curvature in the direction of the unit vector  $\mathbf{q}_y$ , i.e., in the direction of the axis  $oy$ , and  $\mathbf{K}$  = skew-symmetric matrix for the curvature  $\kappa$  in the deformed configuration and given by

$$\mathbf{K} = \begin{bmatrix} 0 & -\kappa \\ \kappa & 0 \end{bmatrix} \quad (8)$$

The rotations from the vectors  $\mathbf{p}_y, \mathbf{p}_z$  to the vectors  $\mathbf{q}_y, \mathbf{q}_z$  can be described using a rotation matrix  $\mathbf{T}$  of a special orthogonal group for two-dimensional finite rotation  $SO(2)$  (Burn 2001; Pi et al. 2003) as

$$\mathbf{q}_i = \mathbf{T} \mathbf{p}_i \quad (9)$$

$$i = y, z$$

or collectively as

$$[\mathbf{q}_y \ \mathbf{q}_z] = \mathbf{T} [\mathbf{p}_y \ \mathbf{p}_z] \quad (10)$$

where the rotation matrix  $\mathbf{T}$  of the special orthogonal Lie group  $SO(2)$  has only one independent parameter, and can be written as

$$\mathbf{T} = \begin{bmatrix} \cos \theta & \sin \theta \\ -\sin \theta & \cos \theta \end{bmatrix} \quad (11)$$

Comparison of Eq. (4) with Eq. (6) leads to

$$\cos \theta = \hat{w}' \quad (12)$$

$$\sin \theta = \hat{v}'$$

Hence, the rotation matrix  $\mathbf{T}$  can be rewritten as

$$\mathbf{T} = \begin{bmatrix} \hat{w}' & \hat{v}' \\ -\hat{v}' & \hat{w}' \end{bmatrix} \quad (13)$$

The rotation matrix  $\mathbf{T}$  in Eq. (13) satisfies the orthogonality condition

$$\mathbf{T} \mathbf{T}^T = \mathbf{I} \quad (14)$$

and the unimodular condition

$$\det \mathbf{T} = +1 \quad (15)$$

Hence, the matrix  $\mathbf{T}$  given by Eq. (13) belongs to the proper orthogonal Lie group  $SO(2)$  for two-dimensional rotation. The components of the matrix  $\mathbf{T}$  become infinite only when  $1 + \epsilon = 0$ , however this situation cannot occur during the deformation of a real composite steel-concrete structure.

Differentiating Eq. (10) with respect to  $z$  produces

$$\left[ \frac{d\mathbf{q}_y}{dz} \quad \frac{d\mathbf{q}_z}{dz} \right] = \frac{d\mathbf{T}}{dz} [\mathbf{p}_y \quad \mathbf{p}_z] \quad (16)$$

Substituting Eqs. (7) and (10) into Eq. (16) and using  $ds^* = (1 + \epsilon)dz$  yields

$$(1 + \epsilon)\mathbf{K} = \frac{d\mathbf{T}}{dz} \mathbf{T}^T \quad (17)$$

and substituting Eq. (13) into Eq. (17) leads to the expression for the curvature in the deformed configuration as

$$\kappa = (1 + \epsilon)^{-1} (\hat{v}' \hat{w}'' - \hat{w}' \hat{v}'') \quad (18)$$

which can be expressed as

$$\kappa = \frac{v'w'' - v''(1 + w')}{[(1 + w')^2 + v'^2]^{3/2}} \quad (19)$$

and which can be simplified further to the familiar expression for the curvature given by

$$\kappa = \frac{-v''}{(1 + v'^2)^{3/2}} \quad (20)$$

if the effect of axial extension  $w'$  is ignored.

Conveniently, the matrix  $\mathbf{T}$  given by

$$\mathbf{T} = \begin{bmatrix} 1 & v' \\ -v' & 1 \end{bmatrix} \quad (21)$$

is often used (Vlasov 1961). In this case, the matrix  $\mathbf{T}$  is still a skew-symmetric matrix but does not satisfy the orthogonal conditions for a rotation matrix that  $\mathbf{T}\mathbf{T}^T = \mathbf{I}$  and  $\det \mathbf{T} = 1$ . After rotation, the basis vectors are not preserved as unit vectors because

$$\mathbf{q}_z \cdot \mathbf{q}_z = \mathbf{q}_y \cdot \mathbf{q}_y = 1 + v'^2 \quad (22)$$

$$\mathbf{q}_y \cdot \mathbf{q}_z = \mathbf{q}_z \cdot \mathbf{q}_y = 0$$

In spite of this, the basis vectors are still assumed to be preserved as unit vectors in the convention analysis. The curvature after deformation then becomes

$$\kappa = -v'' \quad (23)$$

which is a widely used approximation when  $v'^2$  is assumed to be small and when geometric nonlinearity is ignored.

### Position Vectors and Finite Strains

The position vector  $\mathbf{a}_0$  of an arbitrary point  $P$  on the cross section of the member in the undeformed configuration can be expressed as (Fig. 2)

$$\mathbf{a}_0 = \mathbf{r}_0 + y\mathbf{p}_y \quad (24)$$

where  $\mathbf{r}_0$  = position vector of the centroid  $o$  in the fixed axes  $OYZ$ .

In the undeformed configuration, the initial gradient tensor  $\mathbf{F}_0$  can be expressed as

$$\mathbf{F}_0 = \begin{bmatrix} \frac{\partial \mathbf{a}_0}{\partial y} & \frac{\partial \mathbf{a}_0}{\partial z} \end{bmatrix} \quad (25)$$

The position of the point  $P$  in the deformed configuration is determined based on the following two assumptions. First, it is assumed that the composite member is considered to satisfy the Bernoulli hypothesis, i.e., the cross-sectional plane remains plane and perpendicular to the member axis during the deformation except for a slip strain at the interface, and second, the total deformation of a point  $P$  results from two successive motions: translation and finite rotation of the cross section, and a superimposed relative slip displacement between the steel and concrete components along the unit vector  $\mathbf{q}_z$  in the deformed configuration. The slip displacement is given by  $w_{sp}(z)$ . Because slip is the relative axial displacement between the steel and concrete components, the sign of the slip displacement  $w_{sp}(z)$  must be opposite for the steel and concrete components. Under these two assumptions, the position vector  $\mathbf{a}$  of the point  $P_1$ , which is the position of the point  $P$  after the deformation, can be expressed in terms of the basis vectors  $\mathbf{q}_y, \mathbf{q}_z$  as (Fig. 2)

$$\mathbf{a} = \mathbf{r} + y\mathbf{q}_y + \Omega\mathbf{q}_z \quad (26)$$

in which  $\mathbf{r}$  = position vector of the centroid  $o^*$  after the deformation in the fixed axis system  $OYZ$  and is given by Eq. (3), and where

$$\Omega = \begin{cases} -w_{sp} & \text{for the concrete component} \\ w_{sp} & \text{for the steel component} \end{cases} \quad (27)$$

It can be seen that the slip at the interface between the steel and concrete components is considered as an independent degree of freedom, which makes it easier to assign the corresponding proper slip conditions at the connections between composite beams and columns.

In the deformed configuration, the deformation gradient tensor  $\mathbf{F}$  can be expressed as

$$\mathbf{F} = \left[ \frac{\partial \mathbf{a}}{\partial y}, \frac{\partial \mathbf{a}}{\partial z} \right] = \left[ \frac{\partial \mathbf{a}}{\partial y}, (1 + \epsilon) \frac{\partial \mathbf{a}}{\partial s} \right] \quad (28)$$

In this investigation, the well-known strains defined by Love (1927) are used. In this case, the strain tensor can be expressed in terms of the initial and deformation gradient tensors as

$$\begin{bmatrix} \epsilon_{yy} & \frac{1}{2}\gamma_{yz} \\ \frac{1}{2}\gamma_{zy} & \epsilon_{zz} \end{bmatrix} = \frac{1}{2} \{ \mathbf{F}^T \mathbf{F} - \mathbf{F}_0^T \mathbf{F}_0 \} = \frac{1}{2} \{ \mathbf{F}^T \mathbf{F} - \mathbf{I} \} \quad (29)$$

from which the normal strains  $\epsilon_{yy}$  and  $\epsilon_{zz}$  at the point  $P$  are given by

$$\epsilon_{yy} = 0 \quad (30)$$

$$\begin{aligned} \epsilon_{zz} &= \frac{1}{2} \{ [(1 + \epsilon)(1 + y\kappa) + \Omega']^2 + [(1 + \epsilon)\kappa\Omega]^2 - 1 \} \\ &\approx w' + \Omega' + \frac{1}{2}v'^2 + \frac{1}{2}w'^2 + \frac{1}{2}\Omega'^2 \\ &\quad - y[v''(1 + w') - v'w''] + yv''\Omega' \end{aligned} \quad (31)$$

and the shear strains  $\gamma_{yz}$  and  $\gamma_{zy}$  are given by

$$\gamma_{zy} = \gamma_{yz} = \Omega\kappa(1 + \epsilon) = \Omega[v'w'' - v''(1 + \omega')] \approx -\Omega v'' \quad (32)$$

where the third and higher order terms are ignored.

Longitudinal normal stresses that are conjugate to the nonlinear terms  $v'^2/2 + w'^2/2 + \Omega'^2/2$  given in Eq. (31) will produce an

axial stress resultant even under transverse loading because the term  $v'^2/2$  becomes significant as the transverse displacements increase and the term  $(\Omega')^2/2$  also becomes significant when the slip at the interface increases. Hence, the assumption that the resultant of the axial internal forces in the plane of the cross section of a deformed composite beam is equal to zero is correct only when the nonlinear terms  $v'^2/2+w'^2/2+\Omega'^2/2$  are so small that their effects on the longitudinal strain and stress can be ignored.

The shear strains  $\gamma_{zy}$  and  $\gamma_{yz}$  given in Eq. (32) are induced by the interaction of the slip and the in-plane bending and they will vanish for full interaction because  $\Omega=0$ . It is worth pointing out that the shear strains do not appear to be addressed in the open literature. If fact, if geometric nonlinearity is not considered, the nonlinear shear strains  $\gamma_{zy}$  and  $\gamma_{yz}$  will vanish. Because the signs of  $\Omega$  are opposite to each other in the steel and concrete components, the shear stress resultant produced by the shear stresses conjugate to the shear strains may be small. However, the shear stresses play a role in the local yield of steel and concrete and so they should be considered in the FE model. Therefore, the constitutive models for steel and concrete need to be based on both longitudinal normal stresses and the shear stresses induced by the slips at the interface. In the most FE model of beam elements for composite beams and CFT columns, only the longitudinal normal stresses are considered for the constitutive models of concrete and steel.

### Constitutive Model for Structural Steel

The von Mises yield criterion, associated flow rule and isotropic hardening are suitable for structural steel. The von Mises yield criterion can be written as

$$F(\boldsymbol{\sigma}, \lambda) = \sigma_e - \sigma_y = 0 \quad (33)$$

where  $\sigma_y$ =uniaxial yield stress, which describes the change of yield surface for steel. Because the isotropic hardening rule is used,  $\sigma_y$  is given by

$$\sigma_y = \sigma_{y0} + \int_0^{\epsilon_e^{(p)}} H'_s d\epsilon_e^{(p)} \quad (34)$$

where  $\sigma_{y0}$ =uniaxial initial yield stress;  $H'_s$ =hardening parameter for steel; and  $d\epsilon_e^{(p)}$ =equivalent plastic strain rate;  $\sigma_e$ =von Mises equivalent deviatoric stress given by

$$\sigma_e = \sqrt{\frac{3}{2} \mathbf{S} : \mathbf{S}} = \sqrt{\sigma_{zz}^2 + 3\tau_{zy}^2} \quad (35)$$

where the deviatoric stress matrix  $\mathbf{S} = \boldsymbol{\Sigma} + p\mathbf{I}$ ,  $\mathbf{S} : \mathbf{S} = \text{trace}[\mathbf{S}\mathbf{S}^T]$  =double contracted product of  $\mathbf{S}$ ; and  $p$ =effective pressure stress given by

$$p = -\frac{1}{3} \text{trace } \boldsymbol{\Sigma} = -\frac{1}{3} \sigma_{zz} \quad (36)$$

and  $\boldsymbol{\Sigma}$ =stress tensor that can be expressed as

$$\boldsymbol{\Sigma} = \begin{bmatrix} 0 & \tau_{zy} \\ \tau_{zy} & \sigma_{zz} \end{bmatrix} \quad (37)$$

and  $\sigma_{zz}$  and  $\tau_{zy}$ =longitudinal normal and uniform shear stresses in the steel component.

The strain increments can be decomposed into an elastic strain increment and a plastic strain increment as

$$d\boldsymbol{\epsilon} = d\boldsymbol{\epsilon}_e + d\boldsymbol{\epsilon}_p \quad (38)$$

The associated flow and isotropic hardening theory is used for steel. After derivation, the incremental relationship between the stress increment  $d\boldsymbol{\sigma}$  and the strain increment  $d\boldsymbol{\epsilon}$  can be expressed as

$$d\boldsymbol{\sigma} = \mathbf{E}^{(ep)} d\boldsymbol{\epsilon} \quad (39)$$

where  $\mathbf{E}^{(ep)}$ =standard tangent modulus material matrix and given by

$$\mathbf{E}^{(ep)} = \begin{bmatrix} E_s & 0 \\ 0 & G_s \end{bmatrix} - \begin{bmatrix} \sigma_{zz}^2 E_s^2 & 3\sigma_{zz} \tau_{zy} E_s G_s \\ 3\sigma_{zz} \tau_{zy} E_s G_s & 9\tau_{zy}^2 G_s^2 \end{bmatrix} \quad (40)$$

where the coefficient  $\alpha$  is given by  $\alpha = \sigma_e^2 H'_s + \sigma_{zz}^2 E_s + 9\tau_{zy}^2 G_s$ .

It can also be shown that the equivalent plastic-strain rate  $d\epsilon_e^{(p)}$  in Eq. (34) is given by

$$d\epsilon_e^{(p)} = \mathbf{c}^T d\boldsymbol{\epsilon} = \frac{\sigma_e (E_s \sigma_{zz} d\epsilon_{zz} + 3G_s \tau_{zy} d\gamma_{zy})}{\sigma_e^2 H'_s + \sigma_{zz}^2 E_s + 9\tau_{zy}^2 G_s} \quad (41)$$

### Constitutive Model for Concrete

#### Concrete Component

The experimental short term uniaxial stress–strain curve for concrete has essentially no linear range and the slope of the curve is continuous up to “failure.” However, when stresses are less than approximately 35% of the ultimate stress, the stress–strain behavior is almost linear. The concrete component can then be assumed to exhibit an elastic response initially, when it is subjected to compression and shearing. As the stresses increase, some nonrecoverable straining occurs, and the response of the material becomes nonlinear. After the ultimate stress is reached, the material softens until it can no longer carry any stress.

When a uniaxial specimen is loaded into tension, its response is elastic until cracks form so quickly that it is very difficult to observe the actual behavior. For the purpose of modeling, it is assumed that the concrete component that is subjected to tension and shearing loses strength through a softening mechanism and that the open cracks can be represented by a loss of elastic stiffness. It is also assumed that the cracks can close completely when the stress across them becomes compressive.

An isotropically hardening compressive yield surface forms the basis of modeling the inelastic response when the longitudinal normal stresses are dominantly compressive. The constitutive model for the concrete component consists of a compressive yield/flow surface to model the concrete response in the predominantly compressive states of stress, together with damaged elasticity to represent cracks that have occurred at an integration point of the cross section; the occurrence of cracks is defined by a crack detection failure surface and is considered as part of elasticity.

#### Constitutive Model for Tension of Concrete

The crack detection surface for concrete can be defined by (Menetrey and Willam 1995; ABAQUS 2003)

$$F_t(\boldsymbol{\sigma}, \lambda_t) = \sigma'_e - \left(3 - b_0 \frac{\sigma_t}{\sigma_t^u}\right) p' - \left(2 - \frac{b_0 \sigma_t}{3 \sigma_t^u}\right) \sigma_t = 0 \quad (42)$$

where the von Mises equivalent deviatoric stress  $\sigma'_e$  and the effective tensile stress  $p'$  can be obtained from Eqs. (35) and (36) as

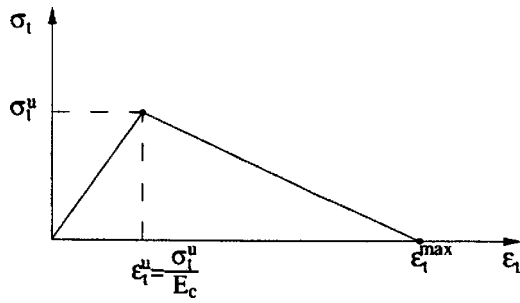


Fig. 3. Tension stiffening model

$$\sigma_e^t = \sqrt{\frac{3}{2} \mathbf{S} : \mathbf{S}} = \sqrt{\sigma_{zz}^2 + 3\tau_{zy}^2} \quad (43)$$

where  $\sigma_{zz}$  and  $\tau_{zy}$  = longitudinal normal tensile and shear stresses in the concrete component; and  $p^t = -\sigma_{zz}/3$ ;  $\sigma_t(\lambda_t)$  = hardening parameter (i.e., the equivalent uniaxial tensile stress), and  $b_0$  = constant and its value can be obtained as (ABAQUS 2003)

$$b_0 = 3 \frac{1 + (2-f)r_t^\sigma - \sqrt{1 + (fr_t^\sigma)^2 + fr_t^\sigma}}{1 + fr_t^\sigma(1-f)} \quad (44)$$

where  $r_t^\sigma$  = ratio of the ultimate stress in uniaxial tension to the ultimate stress in uniaxial compression and given by  $r_t^\sigma = \sigma_t^\mu / \sigma_c^\mu$ , and  $f$  = ratio of the ultimate stress in uniaxial tension to the non-zero principal stress  $\sigma_2$  at the occurrence of cracking when one principal stress has the value  $\sigma_1 = \sigma_c^\mu$  in a plane stress test, i.e.,  $f = \sigma_t^\mu / \sigma_2$ .

Before cracking, the response of the concrete under tensile longitudinal normal and shear stresses is assumed to be linear, and the constitutive equation can be written as

$$d\boldsymbol{\sigma} = \mathbf{E}_{ct} d\boldsymbol{\epsilon} \quad (45)$$

where the stress increment is  $d\boldsymbol{\sigma} = \{d\sigma_{zz}, d\tau_{zy}\}^T$ , the strain increment is  $d\boldsymbol{\epsilon} = \{d\epsilon_z, d\gamma_{zy}\}^T$ , and the tangent material modulus matrix  $\mathbf{E}_{ct}$  is given by

$$\mathbf{E}_{ct} = \begin{bmatrix} E_c & 0 \\ 0 & G_c \end{bmatrix} \quad (46)$$

in which  $E_c$  = Young's modulus of elasticity of the concrete and  $G_c$  = shear modulus of elasticity of the concrete and given by

$$G_c = \frac{E_c}{2(1+\nu_c)} \quad (47)$$

and  $\nu_c$  = Poisson's ratio of the concrete.

After cracking, tensile stresses are generated in the cracked concrete as a result of the transfer, via shear and bond, of the stresses from the reinforcement and steel component. The Gauss point models the crack (or cracks) and the adjacent concrete and consequently its response should be stiffer than it would be for a purely brittle failure. This phenomenon is called "tension stiffening" (Gilbert and Warner 1978). To account for the tension stiffening, the constitutive equation for the cracked concrete can be written in terms of the diminished moduli as

$$d\boldsymbol{\sigma} = \mathbf{E}_{cr} d\boldsymbol{\epsilon} \quad (48)$$

where the damaged tangent material matrix  $\mathbf{E}_{cr}$  is given by

$$\mathbf{E}_{cr} = \begin{bmatrix} E_{cr} & 0 \\ 0 & G_{cr} \end{bmatrix} \quad (49)$$

where  $E_{cr}$  and  $G_{cr}$  = reduced normal and shear moduli.

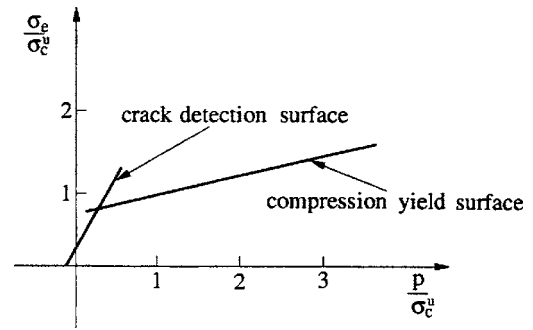


Fig. 4. Concrete failure surfaces in  $(\sigma_e - p)$  plane

The reduced normal modulus  $E_{cr}$  can be determined as (Fig. 3)

$$E_{cr} = \frac{0 - \sigma_t^\mu}{\epsilon_t^{\max} - \epsilon_t^\mu} \quad (50)$$

It is also assumed there are no Poisson effects for open cracks, and so the reduced shear modulus  $G_{cr}$  can be expressed as

$$G_{cr} = \rho G_c \quad (51)$$

$$\rho = \left( 1 - \frac{\epsilon_t}{\epsilon_t^{\max}} \right)$$

where  $\epsilon_t$  = normal tensile strain and  $\epsilon_t^{\max}$  = assumed maximum value of the normal tensile strain.

### Constitutive Model for Compression of Concrete

The compression yield surface for concrete can be defined by (Menetrey and Willam 1995; ABAQUS 2003)

$$F_c(\boldsymbol{\sigma}, \lambda) = \sigma_e^c - \sqrt{3} a_0 p^c - \left( 1 - \frac{a_0}{\sqrt{3}} \right) \sigma_c = 0 \quad (52)$$

where the von Mises equivalent deviatoric stress  $\sigma_e$  is given by

$$\sigma_e^c = \sqrt{\frac{3}{2} \mathbf{S} : \mathbf{S}} = \sqrt{\sigma_{zz}^2 + 3\tau_{zy}^2} \quad (53)$$

where  $\sigma_{zz}$  and  $\tau_{zy}$  = longitudinal normal compressive and shear stresses in the concrete component; and  $p^c = -\sigma_{zz}/3$ , and the constant  $a_0$  can be obtained as (ABAQUS 2003)

$$a_0 = \frac{\sqrt{3}(1 - r_{bc}^\sigma)}{1 - 2r_{bc}^\sigma} \quad (54)$$

where the ratio  $r_{bc}$  is given by  $r_{bc} = \sigma_{bc}^\mu / \sigma_b^\mu$ , with  $\sigma_{bc}^\mu$  being the ultimate stress in biaxial compression and  $\sigma_b^\mu$  being the ultimate stress in uniaxial compression. The typical value  $r_{bc}^\sigma = 1.16$  is usually assumed, and used herein.  $\sigma_c(\lambda)$  = hardening parameter (corresponding to the equivalent anoxia compressive stress in the uniaxial stress strain curve). The compressive yield surface defined by Eq. (52) is plotted together with the crack detection surface defined by Eq. (42) in Fig. 4.

The associated flow rule generally overpredicts the inelastic volume strain. However, for computational efficiency and simplicity, the associated flow and isotropic hardening rules are also used for the concrete component when compression is dominant. While the associated flow assumption is not fully justified by experimental data, it can nevertheless provide results that are acceptably close to these measurements and is therefore used here.

The gradient of the flow potential for the compressive yield surface is

$$\mathbf{a} = \frac{\partial F}{\partial \boldsymbol{\sigma}} = \frac{\partial \sigma_e}{\partial \boldsymbol{\sigma}} - \sqrt{3} a_0 \frac{\partial p}{\partial \boldsymbol{\sigma}} = \frac{1}{\sigma_e} \left\{ \sigma_{zz} + \frac{a_0}{\sqrt{3}} \sigma_e, 3\tau_{zy} \right\}^T \quad (55)$$

The vector  $\mathbf{c}^T$  can be obtained as

$$\mathbf{c}^T = \frac{\mathbf{a}^T \mathbf{E}}{H' + \mathbf{a}^T \mathbf{E} \mathbf{a}} = \frac{\sigma_e [E_c (\sigma_{zz} + a_0 \sigma_e / \sqrt{3}), 3G_c \tau_{zy}]}{\sigma_e^2 H'_c + (\sigma_{zz} + a_0 \sigma_e / \sqrt{3})^2 E_c + 9\tau_{zy}^2 G_c} \quad (56)$$

where  $\mathbf{E}$ =tangent elastic modulus matrix for concrete and given by

$$\mathbf{E} = \begin{bmatrix} E_c & 0 \\ 0 & G_c \end{bmatrix} \quad (57)$$

The stress increments are expressed as

$$d\boldsymbol{\sigma} = \mathbf{E}^{(ep)} d\boldsymbol{\epsilon} \quad (58)$$

where  $d\boldsymbol{\epsilon}$ =vector of strain increments and  $\mathbf{E}^{(ep)}$ =standard tangent modulus material matrix for concrete and can be obtained as (Pi et al. 2006)

$$\mathbf{E}^{(ep)} = \mathbf{E} - \mathbf{E} \mathbf{a} \mathbf{c}^T \quad (59)$$

where the term  $\mathbf{E} \mathbf{a} \mathbf{c}^T$  can be obtained from Eqs. (55)–(57) as

$$\mathbf{E} \mathbf{a} \mathbf{c}^T = \frac{1}{\alpha_c} \begin{bmatrix} \sigma_{zz} + a_0 \sigma_e / \sqrt{3} \sigma_e^2 E_c & 3(\sigma_{zz} + a_0 \sigma_e / \sqrt{3}) \tau_{zy} E_c G_c \\ 3(\sigma_{zz} + a_0 \sigma_e / \sqrt{3}) \tau_{zy} E_c G_c & 9\tau_{zy}^2 G_c^2 \end{bmatrix} \quad (60)$$

in which the coefficient  $\alpha_c$  is given by

$$\alpha_c = H'_c \sigma_e^2 + E_c \left( \sigma_{zz} + \frac{a_0}{\sqrt{3}} \sigma_e \right)^2 + 9G_c \tau_{zy}^2$$

The equivalent plastic strain increment  $d\epsilon_e^p$  can be obtained as

$$d\epsilon_e^p = \mathbf{c}^T d\boldsymbol{\epsilon} = \frac{\sigma_e [E_c (\sigma_{zz} + a_0 \sigma_e / \sqrt{3}) d\epsilon_{zz} + 3G_c \tau_{zy} d\gamma_{zy}]}{\sigma_e^2 H'_c + (\sigma_{zz} + a_0 \sigma_e / \sqrt{3})^2 E_c + 9\tau_{zy}^2 G_c} \quad (61)$$

It is worth pointing out that for CFT columns, particularly for short columns, the confinement effects of the steel tube on the concrete core need to be considered (Hajjar 1998b; Hu et al. 2003). In this case, the hardening parameter  $\sigma_c(\lambda)$  should take the value from the corresponding uniaxial stress–strain curve that includes the confinement effects (Mander et al. 1988).

### Constitutive Model for Crushed Concrete

The total equivalent plastic strain  $\epsilon_e^p$  can be obtained by integrating Eq. (61) and is used as the criterion to detect the crushing of the concrete in compression. When the total equivalent plastic strain  $\epsilon_e^p$  reaches the ultimate strain  $\epsilon^u$  obtained from a uniaxial compression test, i.e.,  $\epsilon_e^p = \epsilon^u$ , the concrete in compression is considered to reach its “crushing” state.

After “crushing,” the concrete is assumed to lose some, but not all, of its strength and rigidity due to the transfer of stresses from the reinforcement and the adjacent uncrushed concrete. The constitutive equation for the “crushed” concrete may be expressed as

$$d\boldsymbol{\sigma} = \mathbf{E}_{cr} d\boldsymbol{\epsilon} \quad (62)$$

where the tangent material matrix  $\mathbf{E}_{cr}$  is given by

$$\mathbf{E}_{cr} = \begin{bmatrix} K & 0 \\ 0 & 0 \end{bmatrix} \quad (63)$$

in which  $K$ =bulk modulus of concrete and defined by

$$K = \frac{E_c}{3(1 - 2\nu_c)} \quad (64)$$

This is consistent with the view of Arnesen et al. (1980) that the instantaneous and complete loss of strength for the crushed concrete is only a crude approximation of real behavior.

### Force–Slip Relationship at Interface

The present FE model provides facility for the incremental relationship between the slip  $w_{sp}$  the corresponding force at the interface (shear force in the case of composite beams and axial transferring force in the case of CFT columns). It is important to input correct the incremental relationship between the slip  $w_{sp}$  and the corresponding force at the interface. The shear force–slip characteristics at the interface of composite steel–concrete beams can be obtained by pushout tests. Several idealized force–slip relationships such as bilinear elastic–full plastic characteristics and rigid–plastic characteristics have been proposed for the design of composite beams (Oehlers and Bradford 1995). However, in order to simulate the experimental curves, the following empirical relationship between the shear force  $Q_{int}$  and the slip  $w_{sp}$  for stud shear connections proposed by Yam and Chapman (1968) is used for composite beams in this investigation:

$$Q_{int} = a[1 - \exp(-bw_{sp})] \quad (65)$$

where  $a$  and  $b$ =constants that are determined by best fitting Eq. (65) with experimental curves. A typical relationship between the shear force and the slip is shown in Fig. 5. The constants  $a$  and  $b$  can be obtained from the two points  $w_{sp2} = 2w_{sp1}$  of the curve as

$$a = \frac{Q_1^2}{2Q_1 - Q_2}$$

and

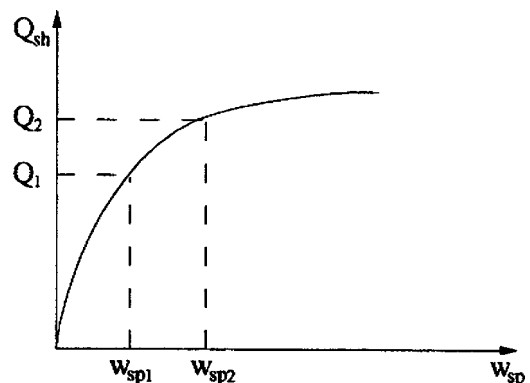


Fig. 5. Load–slip relationship for shear connection between concrete and steel components

$$b = \frac{1}{w_{wp1}} \ln \frac{Q_1}{Q_2 - Q_1} \quad (66)$$

The tangent relationship between the shear force increment and the slip increment can be obtained from Eq. (65) as

$$dQ_{int} = abe^{-bw_{sp}} dw_{sp} \quad (67)$$

It is assumed that the shear connection between the steel and concrete components acts as a continuous medium along the length of an element and that the shear connectors are uniformly distributed along the length of a composite member. Hence, the shear force per unit length (shear flow force)  $q_{sh}$  can be expressed as

$$q_{int} = \frac{Q_{int}}{s} \quad (68)$$

where  $s$ =spacing between the adjacent connectors.

Finally, the incremental relationship between  $q_{int}$  and  $w_{sp}$  can be obtained from Eqs. (67) and (68) as

$$dq_{int} = K_{int} dw_{sp} \quad (69)$$

where  $K_{int}$ =tangent stiffness for slip deformation and given by

$$K_{int} = abe^{-bw_{sp}}/s \quad (70)$$

Experiments focused on the force–slip behavior of CFT columns are limited as pointed out by Hajjar et al. (1998b). Shakir-Khalil (1993a, b) performed an experimental investigation on the force–slip behavior of rectangular CFT sections and proposed a bilinear relationship between the slip and the force transferred. Hence, the incremental relationship between the transferring force and the slip at the interface for CFT columns can also be expressed by Eq. (69) with the tangent stiffness  $K_{int}$  is a constant before the bond between the steel tube and the concrete core is broken down. After bond breaking down, the value of  $K_{int}$  is assumed to vanish. It is worth pointing out that at the connections of frames, the stiffness against slip is usually higher than those obtained from the pushout tests. In this case, the value of  $K_{int}$  can be calibrated directly (Hajjar et al. 1998b).

## Nonlinear Equilibrium

The nonlinear equilibrium equations of an element of a composite steel–concrete member can be derived from the principle of virtual displacements which requires that

$$\delta U = \int_V \delta \boldsymbol{\epsilon}^T \boldsymbol{\sigma} dV + \int_0^l \delta w_{sp} q_{sh} dz - \int_0^l \delta \mathbf{u}^T \mathbf{q} dz - \sum_{k=1,2} \delta \mathbf{u}_k^T \mathbf{Q}_k = 0 \quad (71)$$

for all kinematically admissible sets of infinitesimal virtual displacements  $\{\delta v, \delta w, \delta w_{sp}\}$  where  $l$ =length of the element;  $\delta(\cdot)$ =Lagrange variation operator for infinitesimal changes;  $\boldsymbol{\sigma}$  and  $\delta \boldsymbol{\epsilon}$ =vector of stresses and the vector of the conjugate virtual strains and they are given by

$$\boldsymbol{\sigma} = \{\sigma_{zz}, \tau_{zy}\}^T$$

and

$$\delta \boldsymbol{\epsilon} = \{\delta \epsilon_{zz}, \delta \gamma_{zy}\}^T \quad (72)$$

$q_{sh}$  and  $\delta w_{sp}$ =shear flow force and the conjugate virtual slip at the interface between the steel and concrete components;  $\mathbf{q}$ ,  $\mathbf{Q}_k$ , and  $\delta \mathbf{u}$ =vectors of the external distributed and concentrated loads; and the vector of the conjugate virtual displacements and they are given by

$$\mathbf{q} = \{q_y, q_z, m\}^T$$

and

$$\mathbf{Q}_k = \{Q_y, Q_z, M\}_k^T \quad (k=1,2) \quad (73)$$

and

$$\delta \mathbf{u} = \delta \mathbf{u}_k = \{\delta v, \delta w, -\delta v'\}^T \quad (74)$$

From Eqs. (31) and (32), the vector of the virtual strains can be expressed as

$$\delta \boldsymbol{\epsilon} = \mathbf{S} \mathbf{B} \delta \boldsymbol{\theta} \quad (75)$$

where  $\delta \boldsymbol{\theta}$ =vector of the general virtual displacements and given by

$$\delta \boldsymbol{\theta} = \{\delta v, \delta v', \delta v'', \delta w, \delta w', \delta w'', \delta w_{sp}, \delta w'_{sp}\}^T \quad (76)$$

$\mathbf{S}$ = $2 \times 3$  matrix and is given by

$$\mathbf{S} = \begin{bmatrix} 1 & y & 0 \\ 0 & 0 & 1 \end{bmatrix} \quad (77)$$

and  $\mathbf{B}$ = $3 \times 8$  matrix and given by

$$\mathbf{B} = \begin{bmatrix} 0 & v' & 0 & 0 & 1+w' & 0 & 0 & 1+\Omega' \\ 0 & w'' & -(1+w'+\Omega') & 0 & -v'' & v' & 0 & v'' \\ 0 & 0 & -\Omega & 0 & 0 & 0 & -v'' & 0 \end{bmatrix} \quad (78)$$

The relationships between the infinitesimal increments of the stresses and strains for the steel and concrete given by Eqs. (39), (45), (58), and (62) can be written collectively as

$$\delta \boldsymbol{\sigma} = \mathbf{E}^{(ep)} \delta \boldsymbol{\epsilon} = \mathbf{E}^{(ep)} \mathbf{S} \mathbf{B} \delta \boldsymbol{\theta} \quad (79)$$

where the incremental operator  $d(\cdot)$  is replaced by the variational operator  $\delta(\cdot)$  for consistency in the following formulation because both operators represent infinitesimal changes (called incrementation).

Substituting Eq. (75) into Eq. (71) produces a new expression for the principle of virtual displacements given by

$$\delta U = \int_0^l \delta \boldsymbol{\theta}^T (\mathbf{B}^T \mathbf{R} + \mathbf{q}_{sh}) dz - \int_0^l \delta \boldsymbol{\theta}^T \mathbf{A}^T \mathbf{q} dz - \sum_{k=1,2} \delta \boldsymbol{\theta}^T \mathbf{A}^T \mathbf{Q}_k = 0 \quad (80)$$

where  $\mathbf{R}$ =vector of the stress resultants and is given by

$$\mathbf{R} = \{N, M, Q\}^T = \int_A \mathbf{S}^T \boldsymbol{\sigma} dA \quad (81)$$

in which  $N$ ,  $M$ , and  $Q$ =axial force, bending moment, and shear force, respectively, and given by

$$N = \int_A \sigma_{zz} dA$$

$$M = \int_A \sigma_{zz} y dA$$

and

$$Q = \int_A \tau_{yz} dA \quad (82)$$

$\mathbf{q}_{sh} = 8 \times 1$  vector of the shear flow force acting at the interface between the steel and concrete components and given by

$$\mathbf{q}_{sh} = \{0, 0, 0, 0, 0, 0, q_{sh}, 0\}^T \quad (83)$$

with  $q_{sh}$  being given by Eq. (69);  $\mathbf{A} = 3 \times 8$  matrix and its nonzero elements are given by  $A_{11} = 1$ ,  $A_{22} = -1$ , and  $A_{33} = 1$ .

The general displacement vector  $\boldsymbol{\theta}$  can be expressed as

$$\boldsymbol{\theta} = \mathbf{N}\mathbf{r} \quad (84)$$

where  $\mathbf{N}$  = shape function matrix whose elements are shape functions of  $z$  and  $\mathbf{r}$  = nodal displacement vector and given by

$$\mathbf{r} = \{v_1, v_1', w_1, w_1', w_{sp1}, w_{sp1}', v_2, v_2', w_2, w_2', w_{sp2}, w_{sp2}'\}^T \quad (85)$$

It can be seen that six degrees of freedom are used for each node and that the independent degrees of freedom  $w_{sp}$  and its derivative  $w_{sp}'$  are used to describe slips at the interface between steel and concrete components, which can be conveniently used to assign the slip condition at the connections between beams and columns in the composite structures. It is known that different order of shape functions such as cubic, quintic, or septic functions can be used for the elements of the shape matrix  $\mathbf{N}$ . When higher order shape functions are used, the nodal displacement vector  $\mathbf{r}$  needs to be expanded and stiffness and geometric matrices need to be condensed.

Substituting Eq. (84) into Eq. (80) leads to

$$\delta \mathbf{r}^T \left\{ \int_0^l \mathbf{N}^T (\mathbf{B}^T \mathbf{R} + \mathbf{q}_{sh}) dz - \int_0^l \mathbf{N}^T \mathbf{A}^T \mathbf{q} dz - \sum_{k=1,2} \mathbf{N}^T \mathbf{A}^T \mathbf{Q}_k \right\} = 0 \quad (86)$$

Eq. (86) has to hold for all admissible sets of virtual displacements  $\delta \mathbf{r}$ , so that the nonlinear equilibrium equations can be obtained from Eq. (86) as

$$\int_0^l \mathbf{N}^T (\mathbf{B}^T \mathbf{R} + \mathbf{q}_{sh}) dz - \mathbf{p} = \mathbf{0} \quad (87)$$

where  $\int_0^l \mathbf{N}^T (\mathbf{B}^T \mathbf{R} + \mathbf{q}_{sh}) dz$  = vector of element internal forces while

$$\mathbf{p} = \int_0^l \mathbf{N}^T \mathbf{A}^T \mathbf{q} dz + \sum_{k=1,2} \mathbf{N}^T \mathbf{A}^T \mathbf{Q}_k \quad (88)$$

= vector of external forces acting on the element.

### Consistent Linearization

Consistent linearization of the principle of virtual displacements plays a key role in numerical implementations employing an incremental-iterative solution procedure. A complete account of linearization procedures in the general context of an infinite dimensional manifold can be found in Marsden and Hughes (1978).

Linearization of the principle of virtual displacement can be performed by linearizing Eq. (71), Eq. (80), or more conveniently Eq. (87). Consider an equilibrium configuration  $S$  defined by  $\mathbf{u}$ ,  $\mathbf{q}$ ,  $\mathbf{Q}_k$  ( $k=1,2$ ), and  $\mathbf{q}_{sh}$ , and  $\mathbf{u} + \Delta \mathbf{u}$ ,  $\mathbf{q} + \Delta \mathbf{q}$ ,  $\mathbf{Q}_k + \Delta \mathbf{Q}_k$  ( $k=1,2$ ) and  $\mathbf{q}_{sh} + \Delta \mathbf{q}_{sh}$  define an adjacent equilibrium configuration  $S^*$ . The consistent linearization of the nonlinear equilibrium Eqs. (87) in the equilibrium configuration  $S^*$  can be expressed as

$$\Delta \left[ \int_0^l \mathbf{N}^T (\mathbf{B}^T \mathbf{R} + \mathbf{q}_{sh}) dz - \mathbf{p} \right] = \mathbf{0} \quad (89)$$

where  $\Delta(\cdot)$  = linear incremental operator. The linear incremental operator indicates small variations that are not necessarily infinitesimal. The operational rules for the variational operator  $\delta(\cdot)$  can be used for the linear incremental operator  $\Delta(\cdot)$ .

Eq. (89) can be expanded as

$$\int_0^l \mathbf{N}^T (\Delta \mathbf{B}^T \mathbf{R} + \mathbf{B}^T \Delta \mathbf{R} + \Delta \mathbf{q}_{sh}) dz - \int_0^l \mathbf{N}^T (\Delta \mathbf{A}^T \mathbf{q} + \mathbf{A}^T \Delta \mathbf{q}) dz - \sum_{k=1,2} \mathbf{N}^T (\Delta \mathbf{A}^T \mathbf{Q}_k + \mathbf{A}^T \Delta \mathbf{Q}_k) = 0 \quad (90)$$

From Eqs. (81) and (79)

$$\Delta \mathbf{R} = \int_A \mathbf{S}^T \Delta \boldsymbol{\sigma} dA = \int_A \mathbf{S}^T \mathbf{E}^{(ep)} \mathbf{S} \mathbf{B} \Delta \boldsymbol{\theta} dA = \mathbf{D} \mathbf{B} \Delta \boldsymbol{\theta} = \mathbf{D} \mathbf{B} \mathbf{N} \Delta \mathbf{r} \quad (91)$$

where the familiar property matrix  $\mathbf{D}$  is given by

$$\mathbf{D} = \int_A \mathbf{S}^T \mathbf{E}^{(ep)} \mathbf{S} dA \quad (92)$$

The terms  $\Delta \mathbf{B}^T \mathbf{R}$  can be written as the identities

$$\Delta \mathbf{B}^T \mathbf{R} = \mathbf{M}_\sigma \Delta \boldsymbol{\theta} = \mathbf{M}_\sigma \mathbf{N} \Delta \mathbf{r} \quad (93)$$

The stress matrix  $\mathbf{M}_\sigma = 8 \times 8$  symmetric matrix that accounts for the nonlinear effects of the stress resultants on the tangent stiffness matrix and its nonzero elements are given by

$$\begin{aligned} M_{22} = M_{55} = M_{88} = N \\ M_{26} = M_{62} = -M_{35} = -M_{53} = M \end{aligned} \quad (94)$$

and

$$\begin{aligned} M_{37} = M_{73} = Q \\ M_{38} = M_{83} = M \end{aligned} \quad (95)$$

The term  $\Delta \mathbf{q}_{sh}$  can also be written as the identity

$$\Delta \mathbf{q}_{sh} = \mathbf{M}_{sh} \Delta \boldsymbol{\theta} = \mathbf{M}_{sh} \mathbf{N} \Delta \mathbf{r} \quad (96)$$

where the matrix  $\mathbf{M}_{sh} = 8 \times 8$  matrix with elements  $M_{sh}(i,j) = \delta_{7,j} \delta_{i,7} K_{sh}$  in which  $\delta_{i,j}$  = Kronecher delta and  $K_{sh}$  is given by Eq. (69).

Substituting Eqs. (91) and (93) into Eq. (90) lead to the first term of Eq. (90) as

$$\int_0^l \mathbf{N}^T (\Delta \mathbf{B}^T \mathbf{R} + \mathbf{B}^T \Delta \mathbf{R} + \Delta \mathbf{q}_{sh}) ds$$

$$= \int_0^l \mathbf{N}^T (\mathbf{B}^T \mathbf{D} \mathbf{B} + \mathbf{M}_\sigma + \mathbf{M}_{sh}) \mathbf{N} ds \Delta \mathbf{r} \quad (97)$$

Since the elements of the matrices  $\mathbf{A}$  are constants,  $\Delta \mathbf{A} = \mathbf{0}$ , and the consistent linearization of the second and third terms of Eq. (90) is then obtained as

$$\Delta \mathbf{p} = \int_0^l \mathbf{N}^T \mathbf{A}^T \Delta \mathbf{q} ds + \sum_{k=1,2} \mathbf{N}^T \mathbf{A}^T \Delta \mathbf{Q}_k \quad (98)$$

Substituting Eqs. (84), (97), and (98) into Eq. (90) leads to the tangent stiffness relationship

$$\mathbf{k}_T \Delta \mathbf{r} = \Delta \mathbf{p} \quad (99)$$

where the tangent stiffness matrix  $\mathbf{k}_T$  is given by

$$\mathbf{k}_T = \int_0^l \mathbf{N}^T (\mathbf{B}^T \mathbf{D} \mathbf{B} + \mathbf{M}_\sigma + \mathbf{M}_{sh}) \mathbf{N} ds \quad (100)$$

## Conclusions

A total Lagrangian finite element model for the nonlinear inelastic analysis of composite members was formulated in this paper. The total Lagrangian formulation is directly applicable to the constitutive models expressed in terms engineering stresses and strains, in particular conveniently applicable for the constitutive models for the slips at the interface between the steel and concrete components. A matrix of the special orthogonal group for two-dimensional rotation was expressed in terms of the axial and transverse displacements and their derivatives. The total deformation was assumed to result from two successive motions: displacements and finite rotation of the cross section, and a superimposed relative slip–displacement between the steel and concrete components in the deformed configuration. The nonlinear strain–displacement relationships were then derived based on the rotation matrix and the deformation assumption. The relative slip between the steel and concrete components due to flexible bond at the interface between the steel and concrete components is considered as an independent displacement in the formulation. This makes it easier to assign the corresponding proper slip conditions at the connections between composite frames. The effects of nonlinearities and slip on the deformations and strains in the steel and concrete components and so on the stress resultants (i.e., internal forces), stiffness, and strength of the composite member are thus combined together in the formulation. The shear strains and shear stresses produced by the interaction between the slip and the in-plane bending are included in the FE model.

The constitutive models for steel and concrete are developed in this investigation based on the longitudinal normal stress and the shear stress induced by the slip between the steel and concrete components. Hence, these models include the effects of the slip at the interface on the von Mises yield surface, associated flow rule, and isotropic hardening rule. These constitutive models can be used in association with any type of uniaxial stress–strain curves for steel and concrete, including hot-rolled or cold-formed steel, and confined and unconfined concrete, which will be shown in the companion paper (Pi et al. 2006).

The numerical results in the companion paper (Pi et al. 2006) show the excellent numerical capacity and efficiency of the nonlinear FE model developed in this paper.

## Acknowledgments

This work has been supported by an Australian Research Council Federation Fellowship awarded to the second writer, and a Discovery Project awarded to the second and third writers by the Australian Research Council.

## References

- ABAQUS/Standard user's manual, Version 6.4. (2003). Hibbit, Karlsson & Sorensen Inc., Pawtucket, R.I.
- Ansys Multiphysics 8.0. (2003). Ansys Inc., Canonsburg, Pa.
- Arizumi, Y., and Hamada, S. (1981). "Elastic-plastic analysis of composite beams with incomplete interaction by finite element method." *Comput. Struct.*, 14(5–6), 453–462.
- Arnesen, A., Sørensen, S. I., and Bergan, P. G. (1980). "Nonlinear analysis of reinforced concrete." *Comput. Struct.*, 12(7), 453–462.
- Baskar, K., Shamugam, N. E., and Thevendran, V. (2002). "Finite-element analysis of steel-concrete composite plate girder." *J. Struct. Eng.*, 128(9), 1158–1168.
- Burn, R. P. (2001). *Groups: A path to geometry*, Cambridge University Press, Cambridge, U.K.
- Daniels, B. J., and Crisinel, M. (1993). "Composite slab behaviour and strength analysis. Part I: Calculation procedure." *J. Struct. Eng.*, 119(1), 16–35.
- Gilbert, R. I., and Warner, R. F. (1978). "Tension stiffening in reinforced concrete slabs." *J. Struct. Div. ASCE*, 104(12), 1885–1900.
- Hajjar, J. F., Molodan, A., and Schiller, P. H. (1998a). "A distributed plasticity model for cyclic analysis of concrete-filled steel tub beam-columns and composite frames." *Eng. Struct.*, 20(4–6), 398–412.
- Hajjar, J. F., Schiller, P. H., and Molodan, A. (1998b). "A distributed plasticity model for concrete-filled steel tub beam-columns with interlayer slip." *Eng. Struct.*, 20(8), 663–676.
- Hirst, M. J. S., and Yeo, M. F. (1980). "The analysis of composite beams using standard finite element programs." *Comput. Struct.* 11(3), 233–237.
- Hu, H. -T., Huang, C. -S., Wu, M. -H., and Wu, Y. -M. (2003). "Nonlinear analysis of axial loaded concrete-filled tube columns with confinement effect." *J. Struct. Eng.*, 129(10), 1322–1329.
- Huang, C. -S., et al. (2002). "Axial load behaviour of stiffened concrete-filled steel columns." *J. Struct. Eng.*, 128(9), 1222–1230.
- Lakshmi, B., and Shanmugam, N. E. (2002). "Nonlinear analysis of in-filled steel-concrete composite columns." *J. Struct. Eng.*, 128(7), 922–933.
- Love, A.E. H. (1927). *A Treatise on the Mathematical Theory of Elasticity*. 4th Ed., Dover Publications, New York.
- Mander, J. B., Priestley, M. J. N., and Park, R. (1988). "Theoretical stress-strain model for confined concrete." *J. Struct. Eng.*, 114(8), 1804–1826.
- Marsden, J., and Hughes, T. J. R. (1978). "Topics in the mathematical foundations of elasticity." *Nonlinear analysis and mechanics: Proc., Heriot-Watt Symp.*, R. J. Knops, ed., Vol. II, *Research Notes in Mathematics* 27, Pitman, London.
- Menetrey, Ph., and Willam, K. J. (1995). "Triaxial failure criterion for concrete and its generalization." *ACI Struct. J.*, 92(3), 311–318.
- Oehlers, D. J., and Bradford, M. A. (1995). *Composite steel and concrete structural members—Fundamental behaviour*, Pergamon, Oxford, U.K.
- Pi, Y. -L., Bradford, B. A., and Uy, B. (2003). "Nonlinear analysis of members with open thin-walled cross-section curved in space."

- UNICIV Rep. No. R-414, The Univ. of New South Wales, Sydney, Australia.
- Pi, Y. -L., Bradford, B. A., and Uy, B. (2006). "Second order nonlinear inelastic analysis of composite steel-concrete members. II: Applications." *J. Eng. Mech. Div., Am. Soc. Civ. Eng.* 132(5), 762–771.
- Ranzi, G. (2003). "Composite beams with partial shear interaction." Ph.D. thesis, The Univ. of New South Wales, Sydney, Australia.
- Ranzi, G., Bradford, M. A., and Uy, B. (2004). "A direct stiffness analysis of composite beams." *Int. J. Numer. Methods Eng.*, in press.
- Salari, M. R., Spacone, E., Shing, P. B., and Frangopol, D. (1998). "Nonlinear analysis of composite beams with deformable shear connectors." *J. Struct. Eng.*, 124(10), 1148–1158.
- Schneider, S. P. (1988). "Axially loaded concrete-filled steel tubes." *J. Struct. Eng.*, 124(10), 1125–1138.
- Shakir-Khalil, H. (1993a). "Pushout strength of concrete-filled steel tubes." *Struct. Eng.* 71(13), 230–233.
- Shakir-Khalil, H. (1993b). "Resistance of concrete-filled steel tubes to pushout forces." *Struct. Eng.* 71(13), 234–243.
- Shakir-Khalil, H., and Al-Rawdan, A. (1996). "Composite construction in steel and concrete III." *Proc., Engineering Foundation Conf.*, D. Buckner, and B. M. Shanrooz, eds., Swabian Conference Centre, Germany, 222–235.
- Spacone, E., Filippo, F. C., and Taucer, F. F. (1996). "Fiber beam-column model for nonlinear analysis of R/C frames. 1: Formulation." *Earthquake Eng. Struct. Dyn.*, 25(7), 711–725.
- Thevendran, V., Chen, S., Shamungam, N. E., and Liew, J. Y. R. (1999). "Nonlinear analysis of steel-concrete composite beams curved in plan." *Finite Elem. Anal. Design*, 32, 125–139.
- Vlasov, V. Z. (1961). *Thin-Walled Elastic Beams*, Israel Program for Scientific Translation, Jerusalem.
- Yam, L. C. P., and Chapman, J. C. (1968). "The inelastic behaviour of simply supported composite beams of steel and concrete." *Proc., Inst. Civ. Eng.*, 41(2), 651–683.